Available online at www.sciencedirect.com
SCIENCE DIRECT®
C. R. Geoscience 338 (2006) 237–243
COMPTES RENDUS GEOSCIENCE
http://france.elsevier.com/direct/CRAS2A/

Geomaterials (Sedimentology)

Melting of crustal xenoliths within ascending basalt: Example from the Kula volcanic field, western Anatolia, Turkey

Hasan Bayhan [a], Erkan Aydar [a], Erdal Sen [a], Alain Gourgaud [b,*]

[a] *Hacettepe University, Department of Geological Engineering, 06532, Beytepe, Ankara, Turkey*
[b] *UMR–CNRS 6524, université Blaise-Pascal, 5, rue Kessler, 63038 Clermont-Ferrand, France*

Received 21 January 2004; accepted after revision 12 December 2005

Available online 28 February 2006

Presented by Ždenek Johan

Abstract

During its storage or ascent, basaltic magma inevitably interacts with the surrounding rocks. In this study, schist xenoliths incorporated within ascending basalt are examined. Heating of the xenoliths combined with decompression effect of rapid magma uprise led to dehydration melting of hydrous minerals producing hercynitic spinel, melt, sillimanite and Fe–Ti oxides. The melt is rhyolitic, strongly peraluminous ($1.77 < A/CNK < 2.35$) and corundum normative. It may contain up to 8 wt% FeO_t. It occurs between the foliation planes and in the intragranular environment. Dehydration melting of micas in the schist is probably related to combined effects of heating by basaltic magma and decompression due to the rapid rise. Melting of xenoliths was a progressive process at low pressure. ***To cite this article: H. Bayhan et al., C. R. Geoscience 338 (2006).***

Résumé

Fusion de xénolithes crustaux dans un magma basaltique : exemple de Kula, Anatolie de l'Ouest, Turquie. Durant le stockage ou la montée du magma basaltique, le liquide réagit inévitablement avec les roches encaissantes. À Kula (Ouest anatolien), des xénolithes de schistes ont été modifiés (fusion partielle) par un basalte ascendant. L'élévation de la température et la décompression liées à la montée rapide du magma provoquent un début de fusion des xénolithes, avec déshydratation des minéraux hydratés et production de spinelle hercynitique, liquide rhyolitique et agrégats de sillimanite, verre et oxydes. Le liquide rhyolitique est peralumineux ($1{,}77 < A/CNK < 2{,}35$), à corindon normatif. Il est localisé entre les plans de foliation et dans un environnement intergranulaire. La fusion de xénolithes de schistes, avec déshydratation des micas, a été progressive lors de l'ascension du magma basaltique vers la surface, et s'est développée à faible profondeur. ***Pour citer cet article : H. Bayhan et al., C. R. Geoscience 338 (2006).***

Keywords: Xenolith melting; Hercynite; Rhyolitic glass; Vesicles

Mots-clés : Fusion de xénolithes ; Hercynite ; Verre rhyolitique ; Vésicules

* Corresponding author.
E-mail addresses: eaydar@hacettepe.edu.tr (E. Aydar), gourgaud@opgc.univ-bpclermont.fr (A. Gourgaud).

1631-0713/$ – see front matter
doi:10.1016/j.crte.2005.12.005

Version française abrégée

1. Introduction

L'étude des magmas crustaux a été très utilisée durant ces dernières années pour comprendre la genèse des magmas granitiques et/ou migmatitiques. Des travaux expérimentaux ont été réalisés sur la fusion de roches pélitiques [3,7,12,14,16] et de métagrauwackes [10,13,17]. Quelques travaux ont aussi été réalisés sur des exemples naturels, notamment sur des enclaves de basaltes alcalins [2,4,5,8]. Le point commun pour la génération de liquides siliceux est la fusion et déshydratation non congruente de minéraux hydratés, comme la biotite. Les travaux expérimentaux montrent que la fusion commence entre 780 et 830 °C [14], alors que la température de décomposition de la biotite est de 850 °C [16]. Par ailleurs, comme le magma monte par un conduit vers la surface, la pression diminue, depuis quelques kilobars jusqu'à la pression atmosphérique. Cette chute de pression est à l'origine de l'exsolution des gaz dissous, issus de la fusion des minéraux hydratés, de la nucléation et du grossissement des bulles au sein des produits de fusion [9].

2. Géologie

La région volcanique quaternaire de Kula, en Anatolie de l'Ouest (Turquie), est essentiellement constituée de coulées de laves basaltiques d'origine fissurale et d'appareils monogéniques, de types cônes de scories et maars. Le substratum est composé de roches métamorphiques (schistes, gneiss, marbres) [6]. Dans les produits de projection des cônes de scories, on trouve des enclaves magmatiques (hornblendite, gabbro, lherzolite) et métamorphiques (schistes, gneiss). Il est à noter que les rapports isotopiques de ces basaltes ($^{87}Sr/^{86}Sr$: 0,7030–0,7034) sont bas, ce qui impliquerait l'absence d'une contamination crustale [15], même s'ils contiennent localement des xénocristaux de quartz.

3. Minéralogie

Les xénolithes schisteux présentent des niveaux sombres (liquide magmatique) entre les plans de foliation (Fig. 1). L'assemblage minéralogique (Tableau 1) montre que les schistes contiennent de la sillimanite et du quartz, tandis que les niveaux sombres sont des verres rhyolitiques, avec du spinelle et des produits mélangés (Mix). Ces derniers correspondent à des agrégats de sillimanite, liquide rhyolitique [4], et minéraux opaques qui contiennent un peu de SiO_2 (3–15%) et Al_2O_3 (8–35%). Le verre localisé entre les plans de foliation est aussi observé entre les grains de quartz. Les spinelles sont des hercynites, produits classiques issus de la fusion et déshydratation des biotites [4,10,14].

4. Caractères du liquide

Le verre présente des vésicules de taille variant de 10 μm à 3 mm. Les variations de taille des vésicules sont attribuées à un processus de coalescence des bulles, tandis que la vésiculation est liée à la chute de pression.

Le verre est rhyolitique (ou granitique), peralumineux ($1{,}77 < A/CNK < 2{,}35$) et à corindon normatif. La corrélation SiO_2–Fe_2O_3 est négative (Fig. 2A). Les travaux expérimentaux montrent la croissance des teneurs en silice avec la baisse de température [14] et de pression [10]. Par ailleurs, la comparaison avec les données expérimentales [4,10,12] montre que ce verre est plus potassique et plus siliceux, dans le diagramme de Q–Ab–Or (Fig. 2B).

5. Discussion et conclusion

La fusion de xénolithes crustaux incorporés dans un magma basaltique produit des spinelles hercynitiques, des agrégats minéraux et un liquide rhyolitique. Les agrégats mélangés sont composés de fibrolites et de minéraux opaques. Les travaux expérimentaux montrent que la décomposition des biotites produit les spinelles hercynitiques et cette décomposition nécessite des températures supérieures à 800 °C [11]. La fusion non congruente des biotites est considérée comme un processus majeur pour la genèse des liquides granitiques à pression basse ou intermédiaire [15,16]. La comparaison de la composition du verre avec ceux de la littérature [4,10,12] laisse supposer une genèse sous basse pression (1–3 kbar) et température intermédiaire (850 °C).

En conclusion, la fusion due à la déshydratation des minéraux hydratés des xénolithes de Kula est liée à un processus combiné de réchauffement et de décompression, associé à la montée rapide du magma, qui emballe les xénolithes. La fusion de ces xénolithes est progressive, comme l'attestent la croissance des teneurs en SiO_2 et la concomitance de la vésiculation des verres produits.

1. Introduction

During the last decades, the generation of crustal magmas has become an attractive topic in understanding how granites and/or migmatites form. Most work has been carried out through experimental melting of

pelitic rocks [3,7,10,14,16] and metagreywackes [10, 13,17]. Other investigations focused on natural examples, mainly volcanic xenoliths [2,4,5,8]. It is generally agreed that the incongruent dehydration melting of hydrous minerals, especially micas, governs the melting history and generation of large volumes of silicic melts. The literature debate focuses on melting conditions and phase equilibriums. Experiments show that melting begins between 780–830 °C through the incongruent breakdown of biotite [14], or that total biotite breakdown occurs at about 850 °C [16].

Moreover, dehydration melting of hydrous minerals produces the gas phase contained in vesicles within the melt. As magma ascends through a conduit, the pressure drops from several kilobars to atmospheric pressure, causing exsolution of dissolved gas, bubble nucleation and subsequent growth [9]. The conduit is generally assumed to be rigid, and neglected in mathematical calculations of bubble growth in comparison with the mixture weight [9]. The present study also demonstrates that vesiculation within the glass occurs during/after the dehydration melting of highly foliated metamorphic rock incorporated in ascending basaltic magma (Fig. 1). We report here the occurrence of partially melted schists within alkali basalt and discuss the generation of vesiculated glass and melting-related mineral phases within the schist xenoliths.

2. Geological context of the target

The tectonically extensive Kula region of western Turkey hosts numerous Quaternary fissural basaltic lava flows and monogenetic vents as cinder cones and maars. They overlie the metamorphic basement rocks, which are composed of micaschists, quartz schists, quartz-rich micaschists, gneiss, recrystallised limestones and marbles [6]. Although some magmatic xenoliths (hornblendite, gabbro, lherzolithe, peridodite) and metamorphic xenoliths (schists, gneiss) are present within basaltic cinder tephras, the isotopic ratios ($^{87}Sr/^{86}Sr$: 0.7030–0.7034) of xenoquartz-bearing basalts indicate no significant crustal contamination effects on the basalts [1].

3. Mineral phases and glasses

The well-foliated schist xenoliths have sub-rounded shapes and are occasionally about 10 cm in diameter. Those light-coloured crustal rocks host dark-coloured magmatic-melt-rich layers parallel to the foliation planes (Fig. 1). The dark bands correspond to the melting products including glass, Fe–Ti oxides, while light-coloured bands correspond to the quartz-rich, sillimanite-bearing schist host. The mineral assemblage of partially melted schist mainly consists of quartz (modally: 43%), sillimanite (13%), Fe–Ti oxides (modally: euhedral ones 6%; anhedral oxides: 3%) (Table 1). The rest of the rocks is occupied by vesicle-loaded glass (about 12% in volume). The vesicles within the glass are modally about 22%, whereas the rest of the volume is occupied by 0.5% plagioclase and 0.1 epidote. Some mineralogical analyses give problematic results, for which we use here the term ‘mix’. This name was also used [12] to describe the sillimanite–rhyolitic melt aggregate. In this paper, the term ‘mix’ corresponds either to sillimanite–rhyolitic melt aggregate, or to iron-rich opaque minerals that contain some SiO_2 and Al_2O_3, as seen on Table 1.

Quartz is the main mineral phase of the melted xenoliths, in which it constitutes the light-coloured layers. The quartz grains show resorbed, embayed outlines (Fig. 1c and g).

Sillimanite mostly occurs as elongated prismatic grains exhibiting preferred orientation parallel to the foliation planes. These grains are at the contact with the rhyolitic melt and show little or moderate resorption by melting (Fig. 1c and h). Some fibrolites are also present within the rhyolitic melt (Fig. 1e).

Spinels are mostly euhedral hercynites (Fig. 1d and f) that fill the voids between the foliation planes. The hercynitic spinels are very common products of the incongruent dehydration-melting of the biotite, as shown in [4,10,14], although there is no biotite within our xenoliths (or totally consumed). Some euhedral opaque minerals, although they are optically similar to hercynites, contain in fact SiO_2 (3–15%) and low Al_2O_3 contents (8–35%). Those minerals are interpreted as mix products of the melting.

Glass or rhyolitic composition is abundant either in form of an amorphous aggregate between the foliation layers or as intergranular films between the quartz grains. A deep brown colour characterizes the amorphous aggregates, while the intergranular glass is transparent and isotropic.

4. Melt characteristics

The melt has bubbly character and the size of bubbles is highly variable, ranging from 10 μm to 3 mm, proving that the bubbles grow and coalesce during the rise of magma. The vesiculation of the melt also indicates that during and/or after the melting event the pressure has dropped.

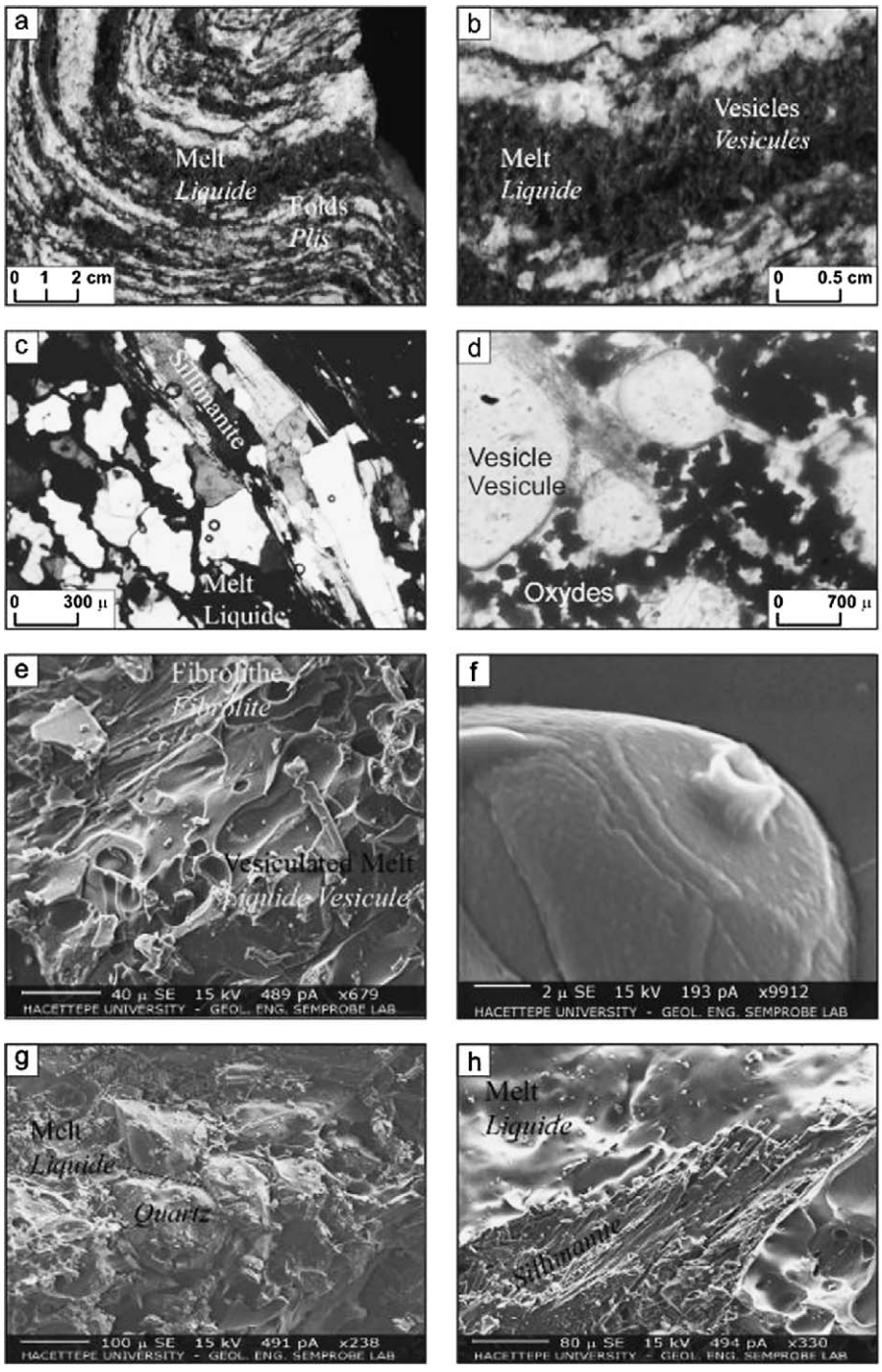

Fig. 1. Illustration of melted schist: (**a**) well-folded thin and thick layers. Dark layers correspond to the melt; (**b**) Zooming on the foliation plane and bubbles; (**c**) Intergranular liquid and bubbles (in crossed nicols, magnification factor: ×125); (**d**) Bubbles and oxides between the foliation plans (in plane polarized light magnification factor: ×650); (**e**) SEM photo of the melt with fibrolites; (**f**) SEM photo of hercynite; (**g**) SEM photo of quartz grains within the melt – note the embayed and resorbed crystal boundaries –; (**h**) SEM photo of melt-sillimanite relationship.

Fig. 1. Illustration de l'évolution de la fusion des schistes : (**a**) alternance de lits épais et de lits plus minces foliés. Les lits sombres correspondent au liquide magmatique ; (**b**) agrandissement de la zone de foliation, avec vésicules dans un lit sombre ; (**c**) liquide et vésicules intergranulaires (lumière polarisée, agrandissement : ×125) ; (**d**) minéraux opaques et vésicules (lumière naturelle, agrandissement : ×650) ; (**e**) photo au MEB du liquide et des fibrolites ; (**f**) photo au MEB de l'hercynite ; (**g**) photo au MEB de grains de quartz dans le liquide. Noter les limites corrodées et résorbées du quartz ; (**h**) photo au MEB des relations liquide–sillimanite.

Table 1
Representative microprobe analysis of participant phases and CIPW norms for the melts (glasses)

Tableau 1
Analyses des phases minérales et des verres avec leurs normes CIPW

	Q	Q	Sill	Sill	Sp	Sp	Sp	Mix	Mix	Mix	Mix	Melt	Melt	Melt	Melt	Melt	Melt	Melt	Melt	Melt	Melt	Melt
Na_2O	0.02	0.03	0.04	0.12	0.02	0.01	0.01	0.04	0.09	0.00	0.19	0.76	0.59	0.71	0.64	0.64	0.50	0.46	0.59	0.71	0.65	0.36
MgO	0.00	0.00	0.00	0.03	0.65	1.19	0.83	9.05	1.27	3.91	0.02	0.91	0.77	0.86	0.85	0.92	0.73	0.38	0.50	0.59	0.83	0.42
K_2O	0.01	0.00	0.07	0.73	0.02	0.01	0.00	0.14	0.41	0.00	1.52	6.17	5.05	5.63	5.15	4.97	4.60	5.09	5.68	5.86	5.60	4.14
CaO	0.00	0.04	0.00	0.03	0.03	0.05	0.01	0.12	0.00	0.06	0.00	0.23	0.34	0.40	0.31	0.26	0.12	0.16	0.22	0.28	0.34	0.12
TiO_2	0.01	0.01	0.00	0.07	1.05	0.83	0.50	0.65	12.45	7.31	0.00	0.56	0.57	0.54	0.60	0.41	0.67	0.39	0.60	0.67	0.55	0.46
$Fe_2O_{3_t}$	0.12	0.08	0.72	1.22	50.52	47.84	48.38	37.82	64.32	52.26	0.67	7.68	6.70	7.92	7.73	7.32	8.33	4.44	5.50	6.52	7.73	4.27
MnO	0.07	0.01	0.06	0.01	0.15	0.13	0.11	0.21	0.08	0.06	0.00	0.02	0.06	0.03	0.00	0.01	0.01	0.01	0.01	0.01	0.08	0.02
SiO_2	99.70	99.67	37.04	39.30	0.05	0.08	0.14	44.57	7.13	3.06	42.98	69.16	70.47	68.41	68.19	71.00	71.81	75.56	73.61	70.17	67.63	75.65
Al_2O_3	0.05	0.04	62.49	57.72	47.04	48.46	49.58	8.58	15.14	33.92	51.32	13.38	13.34	13.91	13.96	12.44	12.41	11.02	13.01	13.76	13.91	10.84
Total	99.97	99.88	100.42	99.21	99.52	98.59	99.55	101.18	100.89	100.58	96.70	98.87	97.89	98.41	97.43	97.96	99.17	97.50	99.72	98.56	97.33	96.28
												C I P W										
Qz												36.98	43.84	38.09	40.48	44.1	47.58	51.32	45.82	40.36	37.95	55.76
Cor												5.05	6.29	5.91	6.77	5.55	6.4	4.47	5.49	5.75	6.15	5.56
Or												36.43	29.83	33.3	30.45	29.36	27.16	30.09	33.57	34.61	33.11	24.44
Ab												6.42	5.03	6.02	5.4	5.38	4.21	3.89	4.96	5.97	5.52	3.05
An												1.13	1.67	1.98	1.53	1.27	0.61	0.78	1.11	1.39	1.71	0.59
En												2.26	1.92	2.13	2.11	2.29	1.81	0.93	1.25	1.47	2.08	1.05
Fs												5.12	4.36	5.43	5.18	4.99	5.28	2.58	3.09	3.96	5.42	2.4
Mt												3.91	3.44	3.98	3.87	3.78	4.32	2.41	2.93	3.35	3.85	2.31
Ilm												1.06	1.08	1.03	1.13	0.78	1.27	0.75	1.15	1.27	1.04	0.87

The analyses were performed by Cameca SX100 instrument at the Blaise-Pascal University, France. Operating conditions were: 15-kV accelerating voltage, 10–12-nA current and 10-s counting time for each element. Q: quartz; Sill: sillimanite; Sp: spinel; Mix: mixture of rhyolitic glass, sillimanite, and oxides; Melt: glass.
Les analyses ont été réalisées à la microsonde Cameca SX100 de l'université Blaise-Pascal, à Clermont-Ferrand, France. Les conditions d'analyse sont les suivantes : tension d'accélération 15 kV, intensité du courant de 10 à 12 nA et temps de comptage de 10 s. Q : quartz ; Sill : sillimanite ; Sp : spinelle ; Mix : mélange verre rhyolitique, sillimanite et oxydes ; Melt : verre.

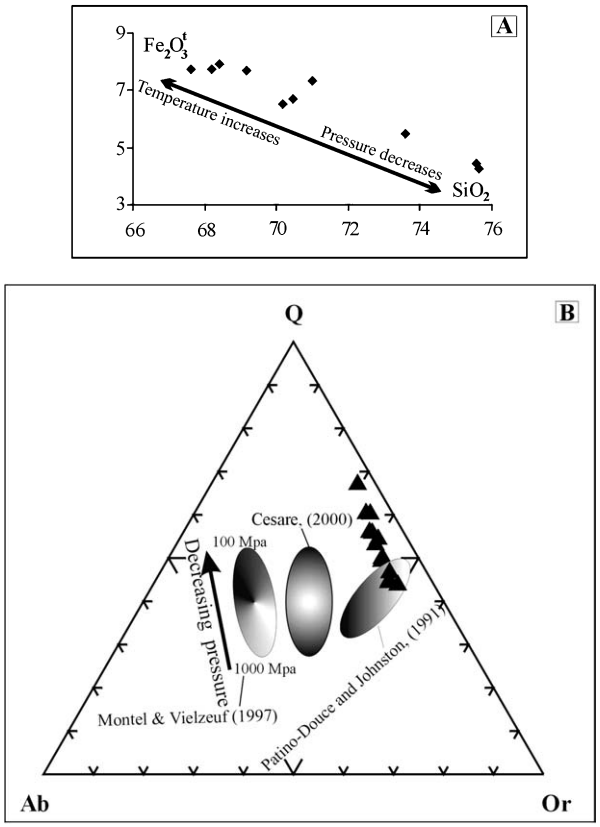

Fig. 2. (**A**) SiO_2–$Fe_2O_3{}^t$ correlation of the melt. (**B**) CIPW normative Q–Ab–Or triangle showing melt compositions of our works (black triangles) and other melts from the literature [4,10,12].

Fig. 2. (**A**) Corrélations SiO_2–$Fe_2O_3{}^t$ pour les verres analysés. (**B**) Comparaison de nos verres (triangles noirs) avec ceux de la littérature [4,10,12] dans le diagramme de Q–Ab–Or normatifs.

The melt is rhyolitic, strongly peraluminous ($1.77 < A/CNK < 2.35$) and corundum normative. The negative SiO_2–$Fe_2O_3{}^t$ correlation of the melt is shown in Fig. 2A. The experimental works on melt production of [14] prove that there is a negative correlation between SiO_2 content and temperature. Additionally, SiO_2 contents of the partial melts decrease with increasing pressure [10]. In this regard, the glasses, poorer in SiO_2 (globally rich in iron) were generated from partial melting of the xenoliths, before higher SiO_2 and lower iron glasses. On the other hand, the Q–Ab–Or triangle with the projection of the glass compositions calculated from the CIPW norm compared to experimental data [4,10, 12] (Fig. 2B) shows that natural glasses are more potassic and more siliceous than experimental glasses derived from the melting of the greywackes [10], but quite similar to melt generated in pelitic system [12]. Assuming that pressure values (1–10 kbar) are significant, we may suppose that the melting of the xenoliths, incorporated by the ascending basalt, occurred at a shallow depth (less than 3 km), close to the surface.

5. Discussion and conclusion

The melting of crustal xenolith incorporated within the basaltic magma produced hercynitic spinels, Fe–Ti oxides and rhyolitic melt. The quenched melt (rhyolitic melt) is iron-rich. Although, there is no biotite within the xenoliths (or totally consumed), the Spl–Sil–Q assemblages are highly suggestive of biotite dehydration melting. Besides, the coexistence of spinel + quartz requires temperatures above 800 °C [11]. The incongruent melting of biotite is considered as the most important cause of simultaneous generation of granitic melts and granulite facies restitic rocks at low to intermediate pressures [15,16]. The rhyolitic melt is peraluminous, corundum normative and similar to S-type granitic composition, however, Na_2O content of rhyolitic melt is very low.

These glasses are potassic, similar to the glass compositions obtained by [1]. Melting may be roughly estimated to occur at low-pressure–intermediate temperatures (Fig. 2B). This hypothesis is also supported by pet-

rographical and textural features (abundance of glass, presence of large vesicles, evidences of bubble growth).

The most interesting point of the xenoliths is the abundant presence of the vesicles. The latter probably indicates that the melting of the xenoliths occurred during the rise of host basaltic magma toward the surface.

Dehydration melting of the hydrous minerals of the xenoliths is probably related to combined effects of either heating of the xenoliths by basalt and/or decompression due to the rapid rise. Melting of xenolith is a progressive process that is expressed by increasing SiO_2 content in the melt, occurrence of intergranular melt (transparent glass) between the quartz minerals in addition to the melt between the foliation plans (dark-coloured melt), chemical change of glass.

Acknowledgements

This work benefited from a research grant of TUBITAK (The Scientific and Technical Research Council of Turkey) (Project No. YDABCAG: 398). The authors thank B. Cesare, J. Dercourt, and J. Touret for suggestions that allowed us to improve the paper.

References

[1] P. Alici, A. Temel, A. Gourgaud, Pb–Nd–Sr isotope and trace element geochemistry of Quaternary extension-related alkaline volcanism: A case study of Kula region (western Anatolia, Turkey), J. Volcanol. Geotherm. Res. 115 (2002) 487–510.

[2] A.J. Brearley, A natural example of the disequilibrium breakdown of biotite at high temperature: TEM observations and comparison with experimental kinetic data, Mineral. Mag. 51 (1987) 93–106.

[3] D.P. Carrington, S.L. Harley, Partial melting and phase relations in high-grade metapelites: an experimental petrogenetic grid in the KFMASH system, Contrib. Mineral. Petrol. 120 (1995) 270–291.

[4] B. Cesare, Incongruent melting of biotite to spinel in a quartz-free restite at El Joyazo (SE Spain): Textures and reaction characterization, Contrib. Mineral. Petrol. 139 (2000) 273–284.

[5] B. Cesare, E. Salvioli Mariani, G. Venturelli, Crustal anatexis and melt segregation in the restitic xenoliths at El Joyazo (SE Spain), Mineral. Mag. 61 (1987) 15–27.

[6] T. Ercan, A. Turkecan, A. Dincel, E. Gunay, Geology of Kula–Selendi area (Manisa), Jeoloji Muhendisligi. Mayis (1983) 3–22.

[7] J.A. Grant, Phase equilibria in partial melting of pelitic rocks, in: J.R. Ashworth (Ed.), Migmatites, Blackie and Son, 1985, pp. 86–144.

[8] R.H. Grapes, Melting and thermal reconstitution of pelitic xenoliths, Wehr volcano, East Eiffel, West Germany, J. Petrol. 27 (1986) 343–396.

[9] O. Melnik, Dynamics of two-phase conduit flow of high-viscosity gas-saturated magma: large variations of sustained explosive eruption intensity, Bull. Volcanol. 62 (2000) 153–170.

[10] J.-M. Montel, D. Vielzeuf, Partial melting of metagreywackes. II. Compositions of minerals and melts, Contrib. Mineral. Petrol. 128 (1997) 176–196.

[11] J.-M. Montel, C. Weber, M. Pichavant, Biotite-Sillimanite-Spinel assemblages in high-grade metamorphic rocks: occurrences, chemographic analysis and thermobarometric interest, Bull. Mineral. 109 (1986) 555–573.

[12] A.E. Patiño-Douce, A.D. Johnston, Phase equilibria and melt productivity in the pelitic system: implications for the origin of the peraluminous granitoids, Contrib. Mineral. Petrol. 107 (1991) 202–218.

[13] A.E. Patiño-Douce, J.S. Beard, Effects of P, $f(O_2)$ and Mg/Fe ratio on dehydration melting of model metagreywackes, J. Petrol. 37 (1996) 999–1024.

[14] G. Stevens, J.D. Clemens, G.T.R. Droop, Melt production during granulite–facies anatexis: experimental data from 'primitive' metasedimentary protoliths, Contrib. Mineral. Petrol. 128 (1997) 352–370.

[15] A.B. Thompson, Dehydration melting of politic rocks and the generation of H_2O-undersaturated granitic liquids, Am. J. Sci. 282 (1982) 1567–1595.

[16] D. Vielzeuf, J.R. Holloway, Experimental determination of the fluid-absent melting relations in the pelitic system, Consequences for crustal differentiation, Contrib. Mineral. Petrol. 98 (1988) 257–276.

[17] D. Vielzeuf, J.-M. Montel, Partial melting of metagreywackes. I. Fluid-absent experiments and phase relationships, Contrib. Mineral. Petrol. 117 (1994) 375–393.